



Neuroradiology/Head and Neck Imaging Review Article

Imaging of the Primary Visual Pathway based on Visual Deficits

Swapnil C. Patel¹, Stephen M. Smith², Alexander T. Kessler², Alok A. Bhatt³

¹Department of Radiology, Atlantic Medical Imaging, Galloway, New Jersey, ²Department of Imaging Sciences, University of Rochester Medical Center, Rochester, New York, ³Department of Radiology, Mayo Clinic, Jacksonville, Florida, United States.



***Corresponding author:**

Alok A. Bhatt,
Department of Radiology, Mayo
Clinic, Jacksonville, Florida,
United States.

bhatt.alok@mayo.edu

Received : 21 January 2021

Accepted : 18 March 2021

Published : 07 April 2021

DOI

10.25259/JCIS_12_2021

Quick Response Code:



ABSTRACT

Vision loss can occur due to a variety of etiologies along the primary visual pathway. Understanding the anatomic organization of the visual pathway, which spans the globe to the occipital cortex, can help tailor neuroimaging to identify the cause of visual dysfunction. In this review, relevant anatomy and optimization of computed tomography and magnetic resonance imaging techniques will be described. This will be followed by a discussion of imaging findings related to pathologies at each functional anatomic level.

Keywords: Vision loss, Optic neuritis, Optic nerve glioma, Papilledema, Craniopharyngioma

INTRODUCTION

Vision loss can result from a broad array of pathologies along the visual pathway. Careful physical examination and anatomical understanding can help localize the site of disease. Visual dysfunction can be generally divided into three anatomic categories: Media (cornea, lens, and globe chambers), retinal, and visual pathways.^[1] Neuroimaging is vital for assessing the visual pathways and primarily relies on computed tomography (CT) and magnetic resonance imaging (MRI), which should be tailored based on the visual deficit [Figure 1 and Table 1]. This article will review the anatomy of the primary visual pathway, optimal imaging technique, and a framework for approaching visual pathway pathology.

ANATOMY

The human visual system begins with the globe, specifically the sclera, uvea, and retina. The retina forms the sensory layer and contains the rod and cone cells (first-order neurons). These specialized neurons synapse with the bipolar cells (second order neurons) which relay signals to the ganglion cells (third order neurons). The axons of the ganglion cells converge at the optic disc to form the optic nerve, which can be subdivided into the intraocular, intraorbital, intracranial, and intracranial segments.^[2] Derived from the forebrain, the optic nerves carry visual information from the retina. The nasal (medial) fibers carry optical information from the bilateral temporal visual fields and then decussate at the optic chiasm. Combined with ipsilateral temporal (lateral) fibers, each optic tract conveys information from the contralateral hemifield of vision [Figure 1].^[2] Fibers of the optic tracts course posterolaterally around the cerebral

This is an open-access article distributed under the terms of the Creative Commons Attribution-Non Commercial-Share Alike 4.0 License, which allows others to remix, tweak, and build upon the work non-commercially, as long as the author is credited and the new creations are licensed under the identical terms.

©2021 Published by Scientific Scholar on behalf of Journal of Clinical Imaging Science

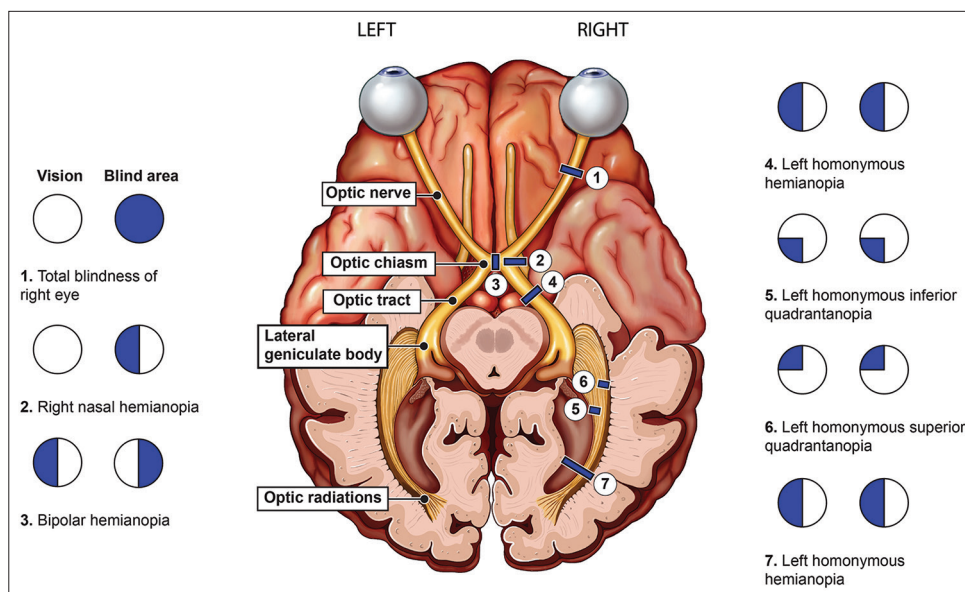


Figure 1: Schematic illustration of the visual pathway and field defects at each topographical location.

Table 1: Localization of visual field deficits.

Visual Field Deficit	Lesion Localization
Monocular vision loss or unilateral central scotoma	Ipsilateral optic nerve
Bitemporal hemianopia	Optic chiasm
Homonymous hemianopia	Contralateral optic tract
Homonymous sectoranopia	Lateral geniculate nucleus
Upper homonymous quadrantanopia	Contralateral temporal optic radiations (Meyer loop)
Lower homonymous quadrantanopia	Contralateral parietal optic radiations
Homonymous hemianopia with macular sparing	Contralateral occipital lobe

peduncles to synapse in the lateral geniculate nucleus (LGN) of the dorsolateral thalamus. Fibers containing superior visual field information synapse within the lateral LGN and fibers containing inferior visual field fibers synapse within the medial LGN. Beyond the LGN, fourth order neurons transmit visual information through the internal capsule in the form of optic radiations. The superior visual field fibers course anterolaterally through the posterior internal capsule, into Meyer’s loop, through the temporal lobe, and terminate in the infracalcarine occipital lobe. The inferior visual field fibers course through the parietal lobe, along the superior aspect of the lateral ventricle, and terminate in the supracalcarine occipital lobe.^[3]

IMAGING TECHNIQUES

CT and MRI are the most common modalities in the evaluation of vision deficits along the visual pathway. CT is often the first-line imaging modality, especially in the acute setting, due to availability and rapid image acquisition. CT can evaluate the bony anatomy of the orbits and skull base,

identify calcifications, delineate fractures, and highlight radiopaque foreign bodies.^[4] CT is typically performed with thin section axial spiral acquisition (0.6–1.25 mm) with the patient instructed to focus on a stationary object to limit radiation to the lens; subsequently, multiplanar reformations can be generated. Intravenous contrast is generally not required unless assessing for inflammatory or neoplastic processes.^[5,6]

MRI offers superior soft-tissue characterization and can serve as a problem solving tool. It offers excellent resolution of the orbit, optic nerve/sheath, optic chiasm, and retrochiasmatic visual pathway. General technique dictates a head and orbit protocol. The orbital component of the exam can maximize resolution by utilizing a specialized coil and narrow field of view. Image acquisition includes thin section (3 mm or less) axial and coronal T1-weighted images, axial T2-weighted images, coronal short tau inversion recovery (STIR) images, and oblique parasagittal images to capture the entire course of the optic nerve. Many institutions have replaced STIR sequences with the Dixon method due to its more uniform fat suppression, high signal-to-noise ratio, and potential to shorten acquisition times. The intracranial component of the exam can be completed with a standard head coil and field of view. Fluid attenuated inversion recovery images, diffusion tensor images, and diffusion-weighted images are important additions to the standard sequences.^[6,7] Before MRI, screening for orbital metallic foreign bodies is essential due to the significant risk for ocular injury from migration and heat.

Imaging can be tailored to focus on the orbits, brain parenchyma, or both depending on the expected site

of pathology within the visual pathway. Angiographic (computed tomography angiogram [CTA] and magnetic resonance angiogram [MRA]) imaging with standard protocols can be obtained to specifically assess for intracranial aneurysm or vascular malformations.^[6]

PATHOLOGY

What follows is a review of common neoplastic, inflammatory, traumatic, and vascular pathologies along the visual pathway.

GLOBE/RETINA

Abnormalities of the globe often result in monocular blindness. Many of the ocular globe pathologies which may lead to blindness such as CMV-induced retinitis, endophthalmitis, and retinal detachment can be diagnosed by ophthalmologic examination and therefore will not be discussed in this article.^[4] Imaging has the potential to aid clinicians in disease processes which extend into the deeper soft tissues. For example, radiologists can readily differentiate between superficial infection (pre-septal cellulitis) versus deeper infections beyond the orbital septum (post-septal cellulitis). Since post-septal cellulitis portends a worse prognosis due to complications (e.g., intracranial extension and cavernous sinus thrombosis), radiologists can assist clinicians in accurately stratifying patient risk and steering patient care beyond the physician exam.

Trauma

Similarly, blunt/penetrating traumatic orbital injury or soft-tissue swelling may limit physical examination and necessitate evaluation with imaging. Thin section orbital CT exam can delineate orbital fractures and associated entrapment syndromes. In addition, CT detects the presence of foreign bodies, lens dislocation, globe rupture, and retinal/choroidal detachment [Figure 2]. Notable pitfalls of globe rupture include intraocular low attenuation areas related to gas tamponade or silicone sponge placement for retinal detachment; these may be misinterpreted as intraocular gas from penetrating trauma. Metallic density from prior scleral band placement may also mimic a foreign body. Evaluation of prior imaging and clinical history can help avoid these pitfalls.^[5] For suspected vascular complications, CTA or MRA can identify cavernous sinus thrombosis or carotid-cavernous fistula (CCF).

Vascular

Transient painless monocular vision loss can occur due to insufficiency/occlusion of the ocular artery or branch vessels. These episodes, referred to as amaurosis fugax,

may represent underlying blood vessel inflammation, atherosclerotic stenosis, or thromboembolic disease. CTA/MRA, vascular duplex ultrasound, or echocardiogram can identify the source and characterize disease extent, guiding appropriate management.^[8] For example, duplex ultrasound can assess for superficial temporal artery wall thickening and edema in giant cell arteritis, the most common primary systemic vasculitis. Giant cell arteritis and other systemic vasculidities can also be detected by mural enhancement of the extracranial and ophthalmic arteries on high resolution 3T MRI.^[9] Finally, CTA or MRA can identify other vascular causes of vision loss including CCF and superior ophthalmic vein thrombosis [Figure 3].^[10,11]

Malignancy

Retinoblastoma, due to sporadic mutation or germline mutation (RB1), is the most common intraocular tumor in children (1 in 15,000 births). Typically presenting as leukocoria in a child (<2 years old), early detection, and treatment can be curative.^[12] In germline mutation cases, there is often bilateral involvement (30–40% cases) and increased risk of pineoblastoma and osteosarcoma.^[6] MRI is the primary imaging modality used to assess disease extent and prognosis; extension beyond the globe increases risk of metastasis and mortality.^[12] Retinoblastoma demonstrates low T2 signal and avidly enhances; this allows recognition of vitreous involvement and extrascleral extension, respectively.^[13] Although CT can readily identify calcifications (present in 85% of cases), there is increased risk of radiation-induced malignancies in patients with germline mutations [Figure 4].^[12]

Ocular melanoma is the most common primary intraocular tumor in adults with a predisposition for Caucasians and older adults. This malignancy arises from the uveal tract and is often found incidentally due to its commonly asymptomatic nature. However, about half of affected patients may report visual field deficits. Local tumor extent and metastatic spread can be assessed with MRI, which demonstrates enhancing lesions with characteristic T1-hyperintense and T2-hypointense signal, related to melanin, and hemorrhage content, respectively.^[13,14]

Metastases from extraocular malignancies, most commonly breast and lung, usually affect the vascular choroid layer. Presenting with progressive pain, diplopia, and visual deficits, metastatic disease is usually enhancing and hypointense on T2-weighted images; it may involve the orbital fat, muscles, and surrounding bone. This pattern of disease can sometimes mimic other benign processes such as thyroid ophthalmopathy or pseudotumor; however, associated choroidal or retinal hemorrhage/detachment suggests metastases.^[15]

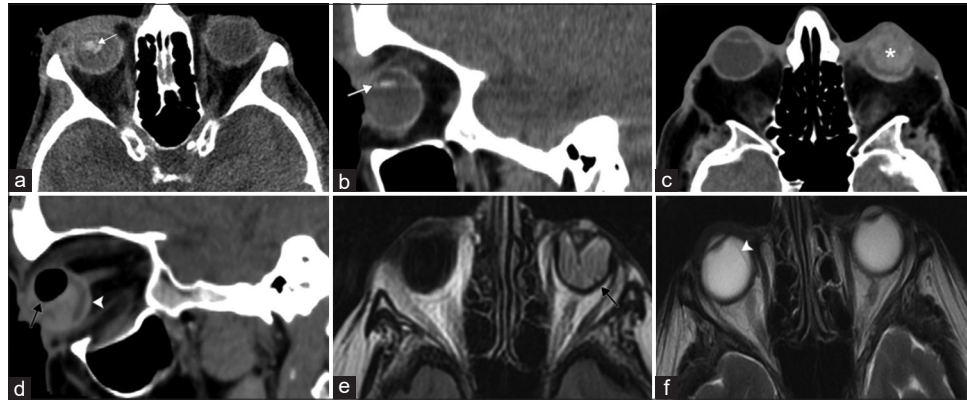


Figure 2: Vision loss at the level of the globe. A 45-year-old patient presents after direct trauma to the right eye with acute monocular right vision loss. (a and b) Axial and sagittal computed tomography (CT) images, respectively, demonstrate right ocular lens dislocation posteriorly and inferiorly (white arrows). A 92-year-old patient presents after direct trauma to the left eye with acute monocular left vision loss. (c and d) Axial and sagittal CT images, respectively, illustrate features of globe rupture including intraocular hemorrhage (asterisk), air (black arrow), and thickened posterior sclera (white arrowhead). (e) Axial T2/Fluid attenuated inversion recovery MR image shows left retinal detachment with folded membranes in the subretinal space (black arrow). (f) Axial T2-weighted MR image displays choroidal detachment in the right eye (white arrowhead).

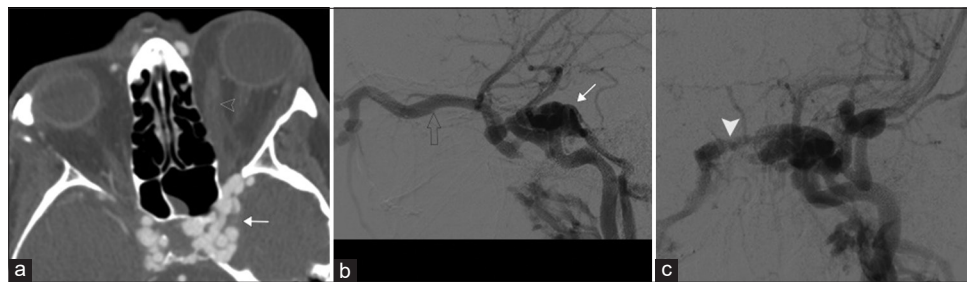


Figure 3: Carotid-cavernous fistula. A 52-year-old female with a history of trauma presents with left globe proptosis. (a) Axial contrast-enhanced computed tomography angiogram, (b and c) lateral and frontal DSA images, respectively, demonstrate a markedly enlarged left cavernous sinus with multiple serpiginous vessels (white arrow) draining a dilated left superior ophthalmic vein (open arrowhead) and intercavernous sinus (white arrowhead). Note the right cavernous sinus is also more full than normal.



Figure 4: Retinoblastoma. A 3-year-old boy presents with leukocoria of the right eye. Axial computed tomography image demonstrates a coarsely calcified intraocular mass in the right eye (arrow). Tumor bulk is predominantly central which is characteristic of the endophytic pattern.

OPTIC NERVE

Inflammation

Optic neuritis is an acute inflammatory condition which can manifest with acute painful vision impairment ranging from blurred vision to vision loss. It is typically unilateral and often accompanied by dyschromatopsia. In young adults, optic neuritis is the most common cause of optic nerve injury. Of these, multiple sclerosis (MS) is one of the most common demyelinating diseases associated with optic neuritis and occurs with a 3:1 female predilection.^[16] Most MS patients will recover functional vision within few weeks, but deficits in color vision, contrast sensitivity, and light brightness may last up to 2 years. If there is bilateral optic nerve involvement (particularly multiple segments or posterior predominance involving the optic chiasm) in an older adult, neuromyelitis optica spectrum disorder should be considered, and presence of the disease specific aquaporin-4 antibodies should be assessed.^[16,17] Gadolinium-enhanced MRI can assess the optic nerves and identify demyelinating plaques within the brain.

The acute phase of disease manifests as increased signal within the center of an enlarged optic nerve on T2/STIR images; contrast enhancement is also present [Figure 5]. The length of optic nerve involvement can be prognostic for visual impairment.^[17,18] In chronic disease, optic nerve atrophy can be appreciated on serial imaging. Other less common diagnostic considerations of optic neuritis include acute disseminated encephalomyelitis, idiopathic optic neuritis, and myelin oligodendrocyte glycoprotein antibody related inflammatory disorder. In the absence of a demyelinating disorder, recurrent optic neuritis can be due to sarcoidosis, paraneoplastic disease, lupus, or chronic relapsing inflammatory optic neuropathy.^[19]

Radiation induced optic neuropathy can occur as a late complication of radiotherapy involving the anterior visual pathway. Risk factors include advanced age, concurrent chemotherapy, previous optic nerve irradiation, or compression. The resultant radiation necrosis typically manifests about 18 months after radiotherapy exceeding 50 Gray. Often contrast enhancement of the optic nerve precedes vision loss. Given the lack of effective treatment, patient selection and dose reduction techniques are essential to minimize this complication.^[20]

Intracranial hypertension

Papilledema can be associated with vision loss and represents optic nerve edema related to idiopathic intracranial hypertension or intracranial mass lesion. Typically identified on ophthalmologic evaluation as swelling of the optic disc, the imaging correlative features include intraocular protrusion of the optic nerve head, enlarged perioptic subarachnoid space, increased optic nerve tortuosity, as well as subtle flattening of the posterior globe [Figure 6].^[7]

Trauma

The optic nerve can be injured during trauma; it is most susceptible to injury at the orbital apex due to traction at the optic canal where it is anchored to the periosteum. Avulsion is most common at the optic head during blunt trauma. Initial evaluation with CT can assess for penetrating foreign bodies and orbital fracture; and MRI can highlight optic nerve contusion and retrobulbar hemorrhage.^[6]

Tumors

Optic nerve gliomas are the most common primary optic nerve tumor, most commonly at the intraorbital segment.^[15] Gliomas can present with visual field deficits or painless proptosis. In neurofibromatosis type (NF) 1, gliomas occur in up to 20% of patients and are commonly bilateral. On MRI, gliomas appear hypointense/isointense on T1-weighted and hyperintense on T2-weighted images with

variable enhancement. The indiscernible optic nerve and lack of calcifications distinguishes the lesion from an optic sheath meningioma.^[15] In NF1 patients, the tumor diffusely buckles and kinks the optic nerve [Figure 7].^[21] In non-NF1 patients, gliomas often demonstrate fusiform morphology, involve the chiasm, and more often lead to vision loss. Treatment is usually limited to progressive gliomas.

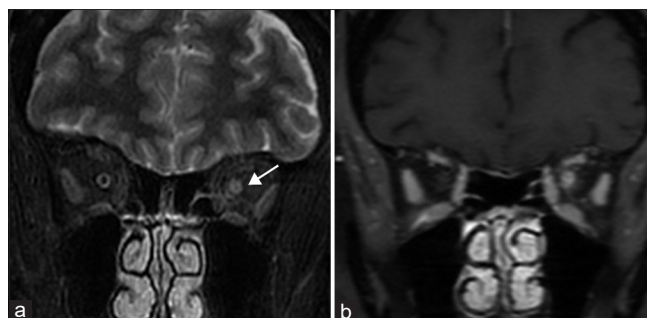


Figure 5: Optic neuritis. A 56-year-old woman presents with left eye pain and blurry vision and papilledema. (a) Coronal STIR MR image demonstrates increased signal within the left optic nerve, consistent with edema (arrow). (b) Coronal T1 post-contrast MR image shows corresponding enhancement.



Figure 6: Idiopathic intracranial hypertension. A 20-year-old woman presents with headaches and papilledema. (a) Axial computed tomography image demonstrates stigmata of intracranial hypertension with subtle intraocular protrusion of the optic heads, more prominent on the left (arrow). (b) Axial T2-weighted MR image more clearly shows intraocular optic head protrusion (arrowheads) with associated prominent perioptic subarachnoid space.

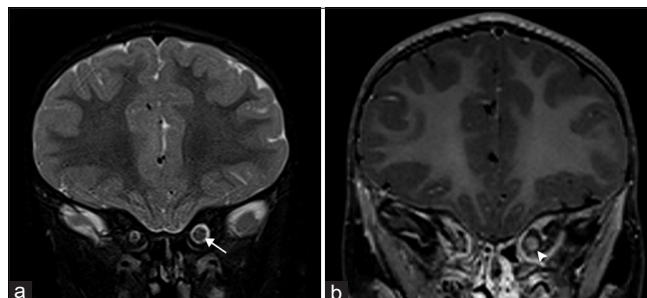


Figure 7: Optic nerve glioma. A 3-year-old patient with neurofibromatosis type 1 who presents with blurred vision. (a) Coronal T2-weighted MR image demonstrates an enlarged left optic nerve (arrow). (b) Coronal T1 post-contrast MR image shows minimal peripheral enhancement (arrowhead).

Primary optic nerve sheath meningiomas exhibit similar behavior and appearance as their intracranial counterparts. They typically present as painless, slowly progressive vision loss in women during their fourth/fifth decade of life.^[15] Bilateral meningiomas may be observed in patients with NF2. Arising from arachnoid cap cells, most are secondary meningiomas which extend into the orbit from an intracranial site. Although both optic nerve gliomas and meningiomas can appear as fusiform enlargement of the optic nerve, CT often highlights the intratumoral psammomatous calcifications and osseous hyperostosis which favor meningioma.^[22] MRI can demonstrate the characteristic “tram-track” appearance derived from the hypointense optic nerve flanked by diffusely enhancing meningioma which often spares the segment immediately posterior to the globe [Figure 8]. Tumor growth can be more aggressive in children and identifying contralateral optic nerve sheath involvement through the optic chiasm or planum sphenoidale is critical to minimize morbidity.^[15]

Lymphoma represents the most frequent primary orbital tumor in older adults. The majority of tumors are unilateral and extraconal; patients present with painless proptosis and restricted orbital movement.^[15] Pain may indicate an aggressive tumor or pseudotumor.^[23] Rapid vision loss suggests diffuse infiltrative involvement of the optic nerve.^[24] The tumors tend to mold around orbital structures and remodel surrounding bone. On MRI, the tumors are isointense to muscle on T1-weighted, hypointense to orbital fat on T2-weighted, and commonly hypointense on apparent diffusion coefficient sequences.^[25] Imaging differentiation between benign and malignant tumors is limited and requires biopsy.

In contrast to lymphoma, inflammatory pseudotumor, also known as idiopathic orbital inflammatory syndrome or non-specific orbital inflammation, is an idiopathic inflammatory condition which presents with painful vision loss and responds to steroids. Although any orbital structure may be



Figure 8: Optic nerve sheath meningioma. An 8-year-old girl with esotropia and exophthalmos of her left eye. (a) Axial T2-weighted fat saturated MR image shows a globular mass encasing the intraorbital segment of the left optic nerve (white arrow). Note the T2 signal of the lesion is similar to brain parenchyma. (b) Axial T1 post-contrast MR image highlights the diffuse tumoral enhancement sparing the encased optic nerve illustrating the tram-track sign (arrowheads). The tumor spares the optic nerve immediately posterior to the globe (black arrow).

affected, symptomatic pseudotumors are typically located at the anatomically narrow orbital apex or optic canal due to compressive perineuritis. Although imaging features of pseudotumor and lymphoma overlap, some studies report that pseudotumors are isointense to orbital fat on T2 sequences compared with hypointensity of lymphoma.^[15] While both pseudotumor and thyroid orbitopathy enlarge the extraocular muscles, pseudotumor also involves the myotendinous junctions [Figure 9].^[7]

OPTIC CHIASM

Bitemporal hemianopia is the classic presentation of compression at the central optic chiasm. Asymmetric lateral involvement of the chiasm can produce ipsilateral nasal field involvement.^[6] Tumors can also extend beyond the optic chiasm to involve the remaining visual system.

Tumors

Gliomas are the most common intrinsic tumor of the optic chiasm and can extend from the optic nerve or hypothalamus to involve the chiasm.^[6]

Sellar and parasellar masses, most commonly pituitary macroadenomas, can compress the optic chiasm. Although symptoms are generally gradual, acute vision loss may develop in the setting of rapid enlargement from intratumoral hemorrhage or necrosis. Macroadenomas generally exhibit similar signal characteristics as gray matter on both CT and MRI. It is critical to describe the position of the optic chiasm relative to the macroadenoma to facilitate surgical planning. However, in aggressive tumors, the optic chiasm may be indiscernible [Figure 10].^[6,26]

Craniopharyngioma is a mixed cystic and solid suprasellar tumor arising from remnants of the Rathke’s cleft along the infundibulum. Imaging features depend on the histologic composition, which include the adamantinomatous and papillary subtypes. Children almost exclusively develop the adamantinomatous subtype with a multilobulated, multicystic morphology, and stippled calcifications. Adults can develop either subtype. The papillary subtype is commonly spherical, predominantly solid, and without calcifications [Figure 11].^[27]

Meningiomas arising from the sellar or suprasellar region can compress the optic chiasm. On CT, they are isodense/mildly hyperdense to gray matter; on MRI, meningiomas are isointense to gray matter on T1 and slightly hyperintense on T2 sequences with diffuse enhancement. Dural tail and adjacent hyperostosis of the bone may be present.^[26]

Metastatic tumors, particularly breast cancer and lymphoma, may involve the pituitary infundibulum leading to visual field deficits and associated diabetes insipidus.^[24]



Figure 9: Idiopathic orbital inflammation (also known as orbital inflammatory pseudotumor). A 39-year-old man with periorbital edema and proptosis which had been worsening for several weeks. (a) Coronal T1 post-contrast MR image shows diffuse intraconal and extraconal enhancement within the left orbit with enlargement of the extraocular muscles (white arrows) and lacrimal gland (white arrowhead); infiltration is visualized around the optic sheath (black arrows). (b) Axial T1 post-contrast MR image shows ill-defined enhancement of the retrobulbar fat (open arrowhead). (c) Axial T1 post-contrast MR image of a different patient shows enhancement of the orbital apex and optic canal segments of the left optic nerve (black arrowhead), a pattern commonly seen in orbital inflammatory pseudotumor.

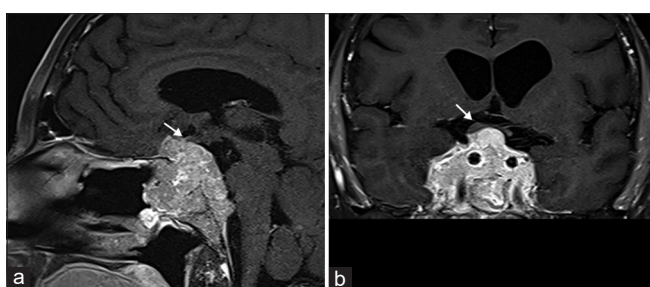


Figure 10: Pituitary Macroadenoma. A 42-year-old male presents with bitemporal hemianopsia. (a and b) Sagittal and coronal T1 post-contrast MR images, respectively, show an enhancing multilobulated mass centered in the sella with extension anteriorly into the sphenoid sinus, inferiorly into the clivus, and superiorly into the suprasellar region. There is mass effect and superior displacement of the optic chiasm (arrows).

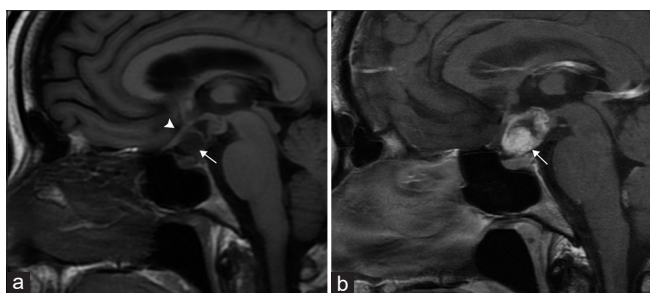


Figure 11: Craniopharyngioma. 50-year-old man with vision changes. (a) Sagittal T1-weighted MR image demonstrates a mixed solid-cystic sellar/suprasellar lesion (arrow), which superiorly displaces the optic chiasm (arrowhead). (b) Sagittal T1 post-contrast MR image demonstrates the predominant solid components of the lesion (arrow).

Vascular

Large intracranial aneurysms arising from the cavernous or supraclinoid segments of the internal carotid artery may

exert mass effect on the optic nerves or chiasm. CTA or MRA imaging can characterize the morphology, size, and extension of aneurysm to determine appropriate management.^[24] CCF with pseudoaneurysm of the cavernous internal carotid artery can cause mass effect on the optic chiasm and cause ipsilateral proptosis [Figure 2].^[24]

OPTIC TRACT

Deficits within the optic tract generally produce contralateral homonymous hemianopia and are most commonly related to posterior extension of pathology around the optic chiasm, medial temporal lobe, or midbrain. The most frequent etiologies include demyelination, infarction, and vascular malformations.^[24]

LGNs

Similar to the optic tract, common pathologies rarely originate within the LGN but spread along the optic tract, thalamus, or medial temporal lobe.^[26] These pathologies classically result in homonymous sectoranopia.^[28] Infarction from occlusion of the choroidal arteries may lead to an isolated deficit of the LGN.

OPTIC RADIATIONS

Optic radiations are white matter tracts susceptible to demyelination, leukoencephalopathy syndromes, radiation injury, or tumoral disruption [Figure 12]. Involvement of the temporal lobe fibers including Meyer's loop produce contralateral homonymous superior quadrantanopia; and involvement of the parietal lobe fibers yields a homonymous inferior quadrantanopia. Posterior involvement leads to more congruous visual field deficits with associated macular sparing.^[6]

VISUAL CORTEX

Pathology occurring within the visual or striate cortex classically produces contralateral homonymous hemianopia with macular sparing. The posterior portion of the cortex is large in volume and represents the fovea; and the anterior cortex represents the peripheral visual field.^[3] Any pathology which crosses the midline may lead to cortical blindness due to bilateral occipital lobe involvement.

Infarcts

Infarction accounts for three-quarters of occipital lobe deficits and may be attributed to occlusion of the middle or posterior cerebral artery, or related to dural venous sinus thrombosis [Figure 13].^[29] Diffusion-weighted imaging can readily identify areas of acute/subacute infarction and

the site of occlusive disease can be identified with CTA or MRA.

Neoplasm

As with the proximal visual pathway, glial tumors, lymphoma, and metastasis are the most common neoplasms to involve the occipital lobes and can be characterized with imaging.^[30]

Vascular anomalies

Arteriovenous malformation or fistula from the occipital artery can become symptomatic due to hemorrhage. Visual field defects depend on the location of abnormal vessels.^[24]

Dysfunctional endothelium and autoregulation in the setting of posterior reversible encephalopathy syndrome often involves the occipital lobes. Patients classically present

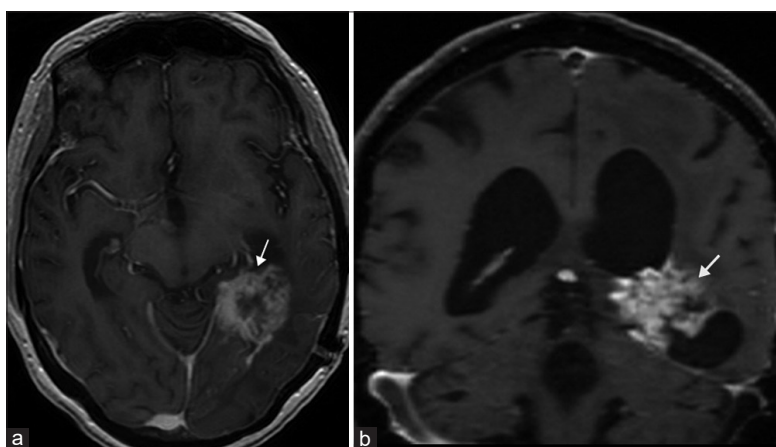


Figure 12: Tumoral disruption of optic radiations. 65-year-old male presented with headache and right homonymous hemianopia, later diagnosed with pathology proven glioblastoma. (a and b) Axial and coronal T1 post-contrast MR images, respectively, demonstrate a heterogeneously enhancing mass situated in the posterior medial left temporal lobe (arrows).

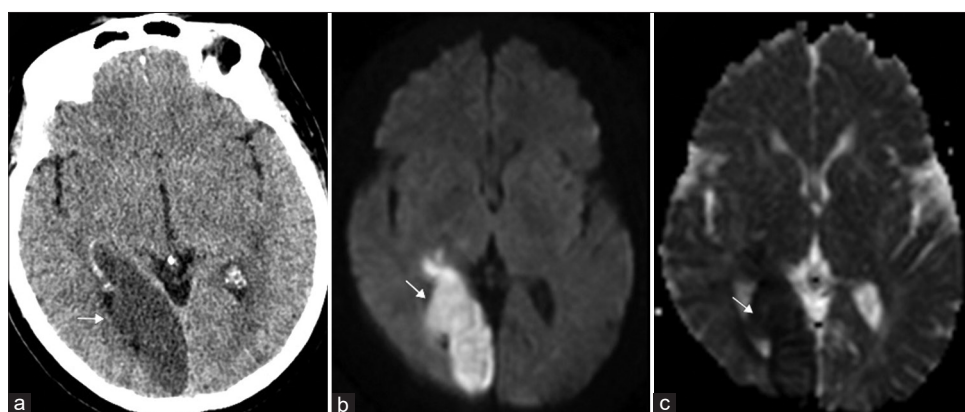


Figure 13: Occipital lobe infarct. 69-year-old woman presented with left homonymous hemianopia. (a) Axial non-contrast head computed tomography illustrates loss of gray-white matter differentiation within the right occipital lobe (arrow). (b and c) Axial DWI (diffusion weighted imaging) and ADC map (apparent diffusion coefficient), respectively, confirm an acute infarct in the right posterior cerebral artery territory (arrows).

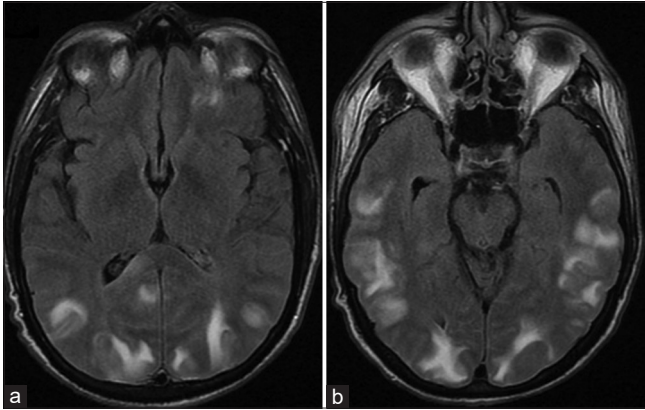


Figure 14: Posterior reversible encephalopathy syndrome. A 52-year-old hypertensive male presents with blurry vision. (a and b) Axial T2/ Fluid attenuated inversion recovery MR images shows areas of increased signal representative of vasogenic edema in the cortex and subcortical white matter predominantly distributed in the posterior cerebral hemispheres bilaterally including the occipital lobes.

with altered mental status and hypertension. This entity can be recognized by the characteristic posterior distribution of increased gyriform signal on T2-weighted imaging representative of vasogenic edema [Figure 14].^[31]

Trauma

Direct traumatic contusion to the occipital lobes can predominantly impact the central macular cortex with resultant bilateral central scotomas.^[24]

CONCLUSION

A variety of neoplastic, inflammatory, traumatic, and vascular processes along the visual pathway can lead to vision loss. Neuroimaging is essential for evaluation of the visual pathway beyond the globe. Clinically, tailored neuroimaging based on anatomy of the visual pathway can help accurately identify pathology and allow the referring provider to treat appropriately.

Declaration of patient consent

The authors certify that they have obtained all appropriate patient consent.

Financial support and sponsorship

Nil.

Conflicts of interest

There are no conflicts of interest.

REFERENCES

1. Bagheri N, Mehta S. Acute vision loss. *Prim Care* 2015;42:347-61.
2. Moore KL, Dalley AF. Optic nerve. In: Moore KL, Dalley AF, editors. *Clinically Oriented Anatomy*. 7th ed. Philadelphia, PA: Lippincott Williams and Wilkins; 2013. p. 1054-83.
3. Wichmann W, Müller-Forell W. Anatomy of the visual system. *Eur J Radiol* 2004;49:8-30.
4. Kim JD, Hashemi N, Gelman R, Lee AG. Neuroimaging in ophthalmology. *Saudi J Ophthalmol* 2012;26:401-7.
5. Kubal WS. Imaging of orbital trauma. *Radiographics* 2008;28:1729-39.
6. Smith MM, Strotzman JM. Imaging of the optic nerve and visual pathways. *Semin Ultrasound CT MR* 2014;35:487-503.
7. Wippold FJ 2nd, Expert Panel on Neurologic Imaging. Orbits, vision, and visual loss. *AJNR Am J Neuroradiol* 2010;31:196-8.
8. Aasen J, Kerty E, Russell D, Bakke SJ, Nyberg-Hansen R. Amaurosis fugax: Clinical, Doppler and angiographic findings. *Acta Neurol Scand* 1988;77:450-5.
9. Geiger J, Ness T, Uhl M, Lagrèze WA, Vaith P, Langer M, *et al.* Involvement of the ophthalmic artery in giant cell arteritis visualized by 3T MRI. *Rheumatology (Oxford)* 2009;48:537-41.
10. LeBedis CA, Sakai O. Nontraumatic orbital conditions: Diagnosis with CT and MR imaging in the emergent setting. *Radiographics* 2008;28:1741-53.
11. Lin KY, Ngai P, Echegoyen JC, Tao JP. Imaging in orbital trauma. *Saudi J Ophthalmol* 2012;26:427-32.
12. de Graaf P, Barkhof F, Moll AC, Imhof SM, Knol DL, van der Valk P, *et al.* Retinoblastoma: MR imaging parameters in detection of tumor extent. *Radiology* 2005;235:197-207.
13. Müller-Forell W, Pitz S. Orbital pathology. *Eur J Radiol* 2004;49:105-42.
14. Balasubramanya R, Selvarajan SK, Cox M, Joshi G, Deshmukh S, Mitchell DG, *et al.* Imaging of ocular melanoma metastasis. *Br J Radiol* 2016;89:20160092.
15. Tailor TD, Gupta D, Dalley RW, Keene CD, Anzai Y. Orbital neoplasms in adults: Clinical, radiologic, and pathologic review. *Radiographics* 2013;33:1739-58.
16. Brusa A, Jones SJ, Plant GT. Long-term remyelination after optic neuritis: A 2-year visual evoked potential and psychophysical serial study. *Brain* 2001;124:468-79.
17. Hickman SJ, Dalton CM, Miller DH, Plant GT. Management of acute optic neuritis. *Lancet* 2002;360:1953-62.
18. Kupersmith MJ, Alban T, Zeiffer B, Lefton D. Contrast-enhanced MRI in acute optic neuritis: Relationship to visual performance. *Brain* 2002;125:812-22.
19. Pula JH, Macdonald CJ. Current options for the treatment of optic neuritis. *Clin Ophthalmol* 2012;6:1211-23.
20. Danesh-Meyer HV. Radiation-induced optic neuropathy. *J Clin Neurosci* 2008;15:95-100.
21. Kornreich L, Blaser S, Schwarz M, Shuper A, Vishne TH, Cohen IJ, *et al.* Optic pathway glioma: Correlation of imaging findings with the presence of neurofibromatosis. *AJNR Am J Neuroradiol* 2001;22:1963-9.
22. Parker RT, Owens CA, Fraser CL, Samarawickrama C. Optic nerve sheath meningiomas: Prevalence, impact, and management strategies. *Eye Brain* 2018;10:85-99.
23. Demirci H, Shields CL, Karatza EC, Shields JA. Orbital

- lymphoproliferative tumors: Analysis of clinical features and systemic involvement in 160 cases. *Ophthalmology* 2008;115:1626-31, 1631.e1-3.
24. Jäger HR. Loss of vision: Imaging the visual pathways. *Eur Radiol* 2005;15:501-10.
 25. Sepahdari AR, Aakalu VK, Setabutr P, Shiehorteza M, Naheedy JH, Mafee MF. Indeterminate orbital masses: Restricted diffusion at MR imaging with echo-planar diffusion-weighted imaging predicts malignancy. *Radiology* 2010;256:554-64.
 26. Ortiz O, Flores RA. Clinical and radiologic evaluation of optic pathway lesions. *Semin Ultrasound CT MR* 1998;19:225-39.
 27. Sartoretti-Schefer S, Wichmann W, Aguzzi A, Valavanis A. MR differentiation of adamantinous and squamous-papillary craniopharyngiomas. *AJNR Am J Neuroradiol* 1997;18:77-87.
 28. Inafuku T, Takagi M, Hoshino H, Segawa H, Sugushita M. Visual field defects in lateral geniculate body infarction. *Jpn J Stroke* 1997;19:323-9.
 29. Zhang X, Kedar S, Lynn MJ, Newman NJ, Biousse V. Homonymous hemianopias: Clinical-anatomic correlations in 904 cases. *Neurology* 2006;66:906-10.
 30. Yang D, Korogi Y, Sugahara T, Kitajima M, Shigematsu Y, Liang L, *et al.* Cerebral gliomas: Prospective comparison of multivoxel 2D chemical-shift imaging proton MR spectroscopy, echoplanar perfusion and diffusion-weighted MRI. *Neuroradiology* 2002;44:656-66.
 31. Lamy C, Oppenheim C, Méder JF, Mas JL. Neuroimaging in posterior reversible encephalopathy syndrome. *J Neuroimaging* 2004;14:89-96.

How to cite this article: Patel SC, Smith SM, Kessler AT, Bhatt AA. Imaging of the Primary Visual Pathway based on Visual Deficits. *J Clin Imaging Sci* 2021;11:19.